ISSN 1068-3755, Surface Engineering and Applied Electrochemistry, 2016, Vol. 52, No. 3, pp. 300–311. © Allerton Press, Inc., 2016.
Original Russian Text © T.Ya. Datsko, V.I. Zelentsov, 2016, published in Elektronnaya Obrabotka Materialov, 2016, No. 3, pp. 83–95.

Fluorine Sorption by Aluminosilicate-Modified Diatomite from Highly Concentrated Fluorine Solutions: 1. Adsorption Equilibrium

T. Ya. Datsko* and V. I. Zelentsov

Institute of Applied Physics, Academy of Sciences of Moldova, ul. Academiei 5, Chisinau, MD-2028 Republic of Moldova
**e-mail: datsko.tatiana@yandex.ru*

Received July 3, 2015; in final form, September 14, 2015

Abstract—The adsorption capacity of natural (D1) and chemically structure-modified diatomite (DMA) in the removal of fluorine ions from highly concentrated fluorine solutions (up to 0.3 mol/L) under static conditions at room temperature is studied. The effect of different parameters—solution pH, initial fluorine concentration, sorbent weight, and particle surface charge density—is examined to determine the adsorption properties of DMA under different process conditions. It is shown that the solution pH plays a crucial role in the removal of fluorine from solutions. An efficient removal of fluorine occurs at a pH of 4.5–5.5. Under equilibrium conditions, upon the saturation of the DMA surface with fluorine ions, the adsorption capacity of DMA achieves 58 mmol/g of sorbent; this value is 5.5 times higher than that of unmodified D1. Fluorine adsorption isotherms for DMA samples are derived; equilibrium adsorption data are modeled using a two-stage Langmuir model; it is shown that the experimental and calculated data on fluorine adsorption are in good agreement: correlation coefficient R^2 for the D1 and DMA samples is 0.9952 and 0.9687, respectively. The fluorine adsorption mechanism is studied. X-ray diffraction and chemical analyses, FTIR spectroscopy, potentiometric titration, and adsorption–desorption experiments reveal that the diatomite–NaF–H_2O system is characterized by the occurrence not only of physical adsorption and ion exchange but also of the chemical bonding of the fluorine ions with the active sites of the sorbent surface, i.e., the formation of weakly soluble fluorine compounds with Al on DMA and with Ca on D1 (AlF_3, Na_3AlF_6, CaF_2).

Keywords: diatomite, modification, adsorption, fluorine, modeling, adsorption mechanism

DOI: 10.3103/S1068375516030042

INTRODUCTION

Fluorine is one of the most common elements of the Earth's crust; various soluble forms of fluorine are present in varying amounts in the atmosphere, water, and soil. A large amount of fluorides is evolved in the production of glass, in the chemical and metallurgical industries, and in the manufacture of semiconductors and integrated circuits. Fluoride or fluorine-containing minerals in rocks and soils are responsible for a high fluorine content in groundwater, which is the main source of drinking water in most regions of Moldova. A small amount of fluorine is necessary for the formation and preservation of teeth in children, whereas high doses of fluoride lead to the development of dental and skeletal fluorosis [1, 2]. Since the fluorine level in drinking water is high and therefore has a harmful effect on people's health, studies on defluorination are of prime importance. According to the World Health Organization, the fluorine concentration in drinking water should not exceed 1.5 mg/L [3, 4]. Hence, for drinking purposes, high fluorine concentrations in natural water must be reduced to the maximum permissible concentration. Despite the fact that the number of studies focused on fluorine removal is increasing every year, the problem remains acute and urgent. Various methods for removing fluorides from water have been tested [5, 6], namely, adsorption, precipitation, electrodialysis, electrocoagulation [7, 8], ion exchange, and reverse osmosis [9]. Among these methods, membrane process and ion exchange are not very common because of the high cost of installation and maintenance, especially in countries with low living standards. Two other methods are more frequently applied, in particular, chemical deposition involving the addition of an aluminum salt–lime mixture into fluorine-contaminated water (Nalgonda technique) [5]. However, the related problems, such as the addition of acids/alkalis in water, residual aluminum, soluble complexes of aluminum fluoride, sludge formation, and relatively high residual fluorine concentrations, are the main obstacles to a wide use of these methods [8–10].

Thus, adsorption is still one of the most commonly used methods of water defluoridation. Activated alumina [11–13] and activated carbon prepared of different materials are appropriate tools for the removal of fluorides and other contaminants from water [14]. However, low rates of adsorption on activated alumina limit the use of this material for processing large amounts of water. The production of activated carbon is expensive; it requires regeneration, which involves technological difficulties and material expenses. Therefore, in recent years, the efforts of researchers have been focused on exploring the possibility of using adsorbents made of inexpensive materials of different types [15–17]. These materials include spent bleaching earth [18], wollastonite, clays, zeolites [18–21], bentonite [22], diatomite [23–25], agricultural products, ash [26, 27], and biosorbents [28].

Over a period of years, the authors have studied the suitability of some inorganic materials for the adsorptive removal of fluorine [29, 30], particularly the fundamental possibility of applying natural mineral raw materials modified by various methods for water defluoridation [31–34].

In this study, the adsorption capacity of a novel sorbent based on local diatomite modified with aluminosilicate compounds (hereinafter, DMA) with respect to fluoride ions from solutions with a high initial concentration (up to 0.3 mol/L) has been examined. The efficiency of fluorine removal by DMA as a function of pH, sorbent dose, and initial fluorine concentration has been determined; adsorption isotherms have been plotted. To understand the adsorption process mechanism, electric surface properties have been studied and X-ray diffraction patterns and FTIR spectra of the samples have been recorded.

Generally, it is difficult to understand surface phenomena in natural mineral sorbent–inorganic anion systems on a molecular level because of the internal complexity and heterogeneous nature of the composition, mineralogy, and morphology of the adsorbent. An attempt to contribute to the understanding of fluorine adsorption by DMA has been made in this study.

For comparison, all experiments are repeated using the unmodified material, i.e., original diatomite (hereinafter, D1).

ADSORPTION MODELS

To determine some adsorbent characteristics, such as maximum adsorption capacity and equilibrium constant, isotherms are typically modeled in terms of known adsorption models and the most appropriate model is selected on the basis of the curve shape and the linear regression coefficient criteria (maximum R^2 value). The Langmuir, Freundlich, BET (for solutions), and Redlich–Peterson isotherm models are the best-known and most commonly used models for adsorption from solutions. Each of these empirical models has its own background and justification; therefore, in the case of good agreement with the experimental curve, it is possible to make an indirect conclusion about the processes that occur during adsorption on the sorbent surface and about the nature of adsorption.

Most of the studies focused on fluorine removal by mineral sorbents addressed fluorine adsorption from solutions with low initial concentrations; the isotherm shapes were quite satisfactorily described in terms of the above models. However, in the case of high initial concentrations, the isotherms have a more complex shape which cannot be modeled using one of these models. The authors of [35] effectively described the S-shaped isotherm of fluorine adsorption by layered double hydroxides $MgAl–CO_3$ in terms of the Langmuir–Freundlich model. In other studies focused on fluorine adsorption by aluminum and iron oxides [36], the formation of two-step isotherms was observed; however, modeling was not applied to describe those isotherms.

In some cases, the occurrence of two-step isotherms is attributed to interactions between the adsorbed molecules. These interactions (multilayer adsorption, stereochemical interaction) cause the stabilization of an adsorbate on a solid surface and, thereby, lead to an increase in the affinity of the surface to the adsorbate and an increase in the surface excess thereof [37]. Another concept stemming from models for a saturated adsorption medium takes into account the heterogeneity of the adsorbent surface with allowance for two or more sites with different adsorption energies [38]. To describe multilayer adsorption, more complicated equations, such as the BET equation, were proposed [39, 40]. However, numerical methods of recent years cannot easily be used because of a large number of mandatory parameters, which makes the model too complex for practical calculations at a reasonable number of experiments.

The available published data [41–43] suggest that these multistep isotherms should be described using a nonlinear mathematical model based on the summation of Langmuir isotherms and an additional assumption that the sorbent surface comprises sterically or energetically heterogeneous adsorption sites and the adsorbed molecules can interact between each other.

Since adsorption involves the sorbate–sorbent interfacial interaction, the surface properties of the sorbent play an important role in the sorption process. The surface functional groups of the mineral are binding sites for sorption reactions. A surface functional group is "a chemically reactive molecular unit bound to the structure of a solid at its periphery such that the reactive components of the unit can be bathed by a fluid" [37]. Surface molecules have fewer nearest neighbors than molecules in the bulk and are not fully coordinated. Once a mineral is brought into contact

Table 1. Chemical composition of diatomite before and after modification

Sample	Composition, %						Calcination loss, %
	SiO_2	Al_2O_3	Fe_2O_3	CaO	MgO	$Na_2O + K_2O$	
D1	59.70	1.31	1.28	12.80	0.69	0.34	18.5
DMA	35.50	18.90	1.33	9.00	9.02	1.30	10.3

with water, hydroxyl functional groups (OH^-) are formed on the surface. This event is attributed to chemisorption and subsequent hydrolysis of water molecules on the sorbent surface.

The surface charge of the sorbent is dependent on the pH of the surrounding aqueous solution. Neutral or alkaline pH conditions generally lead to the development of a negative surface charge. Accordingly, under acidic conditions, excess protons are typically retained by the surface, resulting in the development of a total positive surface charge [44]:

$$\underset{\text{Low pH}}{XOH_2^+} \leftarrow XOH \rightarrow \underset{\text{High pH}}{XO^-}.$$

It is important to keep in mind that, at almost any pH value, positively, negatively, and neutrally charged sites are distributed on the sorbent surface. At a certain average pH, which is referred to as the point of zero charge (PZC), the total surface charge is zero:

$$\left[XOH_2^+\right] = \left[XO^-\right].$$

Surface charge can have an effect on the distribution of neighboring solutes in such a way that a decrease in pH of the surrounding aqueous solution will contribute to the attraction of anionic compounds from the solution to the surface, i.e., to their adsorption [45].

The PZC of D1 and DMA was determined by potentiometric titration at different ionic strengths of the background electrolyte (accordingly, at different thicknesses of the electric double layer) [46, 47]. In the case of diatomite, the PZC is given by the proton conditions in solution under which the surface charge caused by the adsorption of H^+ or OH^- ions is zero ($\sigma_0 = 0$). The point at which the surface charge is no longer dependent on the ionic strength is the point of intersection of three potentiometric titration curves recorded at three different ionic strengths of the solution; the pH corresponding to this point is pH_{PZC}.

EXPERIMENTAL

Materials and Methods

All the chemical reactants used were of analytical and reagent grades. Bidistilled water was employed in all experiments. All experiments, except for experiments on the effect of solution temperature on the adsorption rate and the adsorption isotherm, were conducted at room temperature and normal atmospheric pressure.

The initial synthetic fluoride solution was prepared by the addition of an appropriate amount of sodium fluoride to distilled water and then used for adsorption experiments after adequate dilution.

DMA Synthesis

Natural diatomite from a field in the village of Viscauti (Orhei region, Republic of Moldova) was used in this study.

Diatomite samples (15 g) were introduced into 100 mL of a 3 M NaOH solution; the mixture was stirred at 55°C for 40 min and then centrifuged; the precipitate was introduced into 100 mL of 2 M aluminum sulfate; the resulting mixture was held at room temperature under constant stirring for 5 h. After centrifugation, the filtrate was removed and the precipitate was exposed to a concentrated ammonia solution at room temperature for 5 h and then centrifuged; the resulting precipitate was separated from the filtrate, washed with distilled water, air-dried at 110°C, and stored in a desiccator at room temperature until use.

The aluminum content in the samples was determined by atomic absorption spectrophotometry using an AAS3 1N instrument. Before this analysis, the samples were dissolved in 6 M HCl to transfer the precipitated aluminum compounds into solution.

Table 1 shows the silica analysis results for the D1 and DMA samples.

The phase composition of D1 and DMA was identified by diffractometric analysis on a DRON-3M X-ray diffractometer using FeK_α radiation at U/I = 30/30 and measurement limits of 2×10^2 to 5. The slit width was 1–1–1–0.25.

The textural characteristics of the D1 and DMA samples—specific surface area, pore size and volume, and pore size distribution—were determined by the BET method from low-temperature nitrogen adsorption (the nitrogen molecule area was assumed to be 0.162 nm^2) on a Micrometrics ASAP2000 instrument; the sample weight was about 0.2 g. Before nitrogen adsorption, the samples were degassed at 473 K in a vacuum of 5×10^{-4} atm for 4 h to remove the entire adsorbed moisture from the surface and pores of the sample.

Transmission spectra were recorded on a Perkin-Elmer Spectrum-100 FTIR spectrometer in vaseline oil.

Determination of the PZC of the Samples

Before and after fluorine adsorption from a solution with an initial fluorine concentration of 0.035 mol/L, 10 g/L of D1 and DMA was introduced into a background electrolyte solution (0.001, 0.01, and 0.1 M potassium chloride solutions) and allowed to stand at room temperature under stirring for 24 h. After that, the suspensions were titrated with 0.1 M HCl and KOH solutions under continuous monitoring of pH. Solution volumes required for pH transition from an alkaline to acidic region and back were determined. Measurements were conducted three times; the result was the average of three readings.

Surface charge density is determined as follows:

$$\sigma_0 = \frac{FC\Delta V}{mS_{sp}} \times 100,$$

where σ_0 is the surface charge density, $\mu K/cm^2$; F = 96500 K/g-equiv (9.6×10^{10} = μK/g-equiv); C is the concentration of HCl or KOH, g-equiv/cm^3 (0.01 N); ΔV is the amount of added HCl or KOH, cm^3; m is the sorbent weight, g; and S_{sp} is the specific surface area, m^2/g.

The σ_0–pH curves for three ionic strengths for all the diatomite samples were plotted. The points of intersection of three titration curves were marked as pH_{PZC}.

Fluorine Adsorption by DMA

Adsorption experiments were conducted under steady-state conditions: 0.2 g of the adsorbent (D1 and DMA) was introduced into 50 mL of a sodium fluoride solution in an acetate buffer with an initial fluorine content of 5×10^{-4} to 0.3 mol/L; the mixture was stirred at a speed of 350 rpm for 2 h; this time interval was previously determined as the equilibration time. Upon the establishment of equilibrium, the fluorine concentration was measured using an ELIS 131F fluoride-selective electrode and an I160-M ionomer. Each experiment was conducted twice under identical conditions. The standard deviation of the measurements was within ±3%.

The necessity of conducting an experiment with a buffer solution was imposed by a change in the solution pH during sorption, especially in the first few minutes. Table 2 shows some results of changes in the pH of the diatomite sample suspension after 10-min stirring with water and sodium fluoride.

Similar observations were made in a study of fluorine adsorption by clay minerals and hydrated alumina from a 0.1 M solution: after a 3-h fluorine adsorption, the resulting pH value increased for all suspensions, especially for that of alumina (from 7.3 to 9.6) [48].

Table 2. Change in the solution pH during fluorine adsorption by the D1 and DMA samples

Sample	Suspension pH after 10-min stirring	
	with water, pH ~ 6.5	with a NaF solution, pH ~ 7.2
D1	8.3	8.9
DMA	7.5	11.5

Table 3. Characteristics of D1 and DMA responsible for the adsorption properties of the diatomites

Sample	D1	DMA
Specific surface area, m^2/g	37.54	81.77
Sorption pore volume, cm^3/g	0.0442	0.1058
pH_{PZC}	8.34	8.85
a_m, mmol/g	10.5	58.0

RESULTS AND DISCUSSION

Table 3 shows some characteristics of the diatomite samples that are responsible for their adsorption properties.

The physicochemical characteristics of D1 and DMA are discussed in detail in [49].

Effect of Solution pH on Fluorine Removal

The main factor governing the adsorption at the aqueous electrolyte solution–absorbing mineral surface interface is pH. Preliminary experiments revealed that the pH of the maximum fluorine adsorption lies in a narrow range (4.5–5.5) for DMA, while the fluorine adsorption by D1 is weakly dependent on the solution pH.

Figure 1 shows the adsorption of fluoride ions by D1 and DMA as a function of the solution pH. The fluorine adsorption by DMA is maximal at a pH of 4.5–5.5 and decreases with a further increase in pH. Hence, the defluoridation ability of the adsorbent is maximal in the acidic range. An abrupt decrease in the adsorption capacity with increasing pH can be attributed to the competitive adsorption of hydroxyl ions and fluoride in this pH range.

In the case of D1, the fluorine adsorption remains constant to a pH of 7 and then slightly decreases. In the maximum adsorption range, the magnitude of fluorine adsorption by DMA considerably exceeds the magnitude of fluorine adsorption by the original sample; however, at a pH above 7.5, it decreases; at a pH of 9, it is close to zero.

An increase in the solution pH during adsorption suggests that the surface hydroxyl groups penetrate into the solution instead of fluoride ions, which bind to aluminum ions in the mineral lattice. This pro-

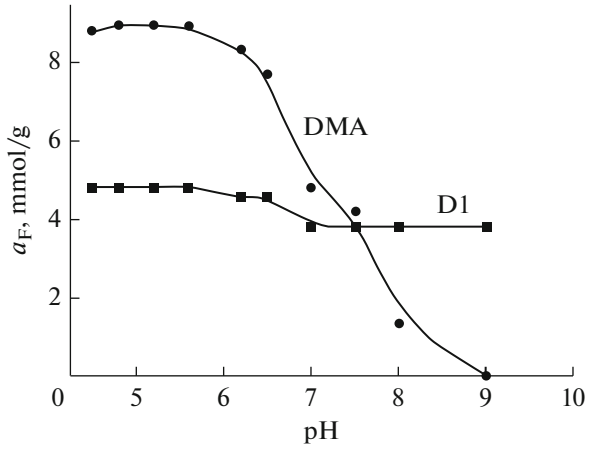

Fig. 1. Dependence of the fluorine adsorption by the D1 and DMA samples on the solution pH.

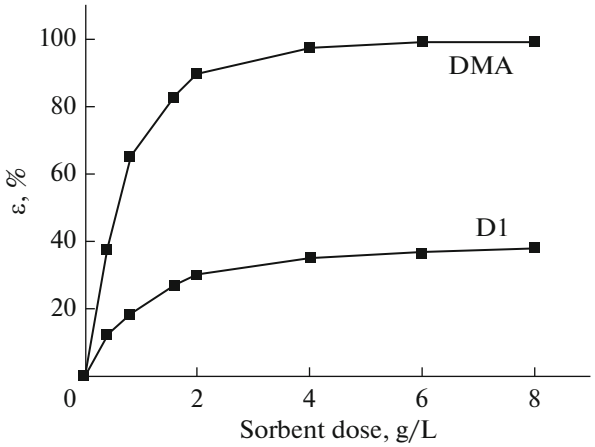

Fig. 2. Effect of the sorbent dose on the fluorine extraction by the D1 and DMA samples at an initial fluorine concentration of 0.0345 mol/L, a solution pH of 5.0 ± 0.5, and an equilibration time of 120 min.

cess is associated with the dissolution of aluminum [36, 50, 51]. The amount of adsorbed fluorine depends on the amount and accessibility of Al–OH bridges: more readily accessible aluminum ions dissolve much more rapidly and coordinate six F^- ions in solution. The removal of the aluminum ions leads to the release of OH^- ions for substitution by fluoride ions. It should be noted that the amounts of released hydroxyls and adsorbed fluoride ions are far from being equivalent. The dissolution and substitution do not last infinitely long. If the solution alkalinity is constantly neutralized by an added acid, then, over time, the release of hydroxyls slows down and the reaction wanes. It is clear that the adsorption capacity of the sorbent with respect to fluorine is dependent on excess surface Al–OH bonds; the more developed the adsorbent pore structure providing a large active surface, the higher the adsorption capacity of the adsorbent, as evidenced by the data in Table 3 and Fig. 1.

The weak dependence of fluorine adsorption on the solution pH that was observed for the D1 sample can be explained in terms of the concept of the buffer capacity of the surface Si–OH groups of diatomite particles according to the reaction [48]

$$>Si{-}OH + OH^- \rightarrow >Si{-}O^- + H_2O.$$

Effect of Sorbent Dose on Fluorine Adsorption

To determine optimum conditions for fluorine adsorption, the effect of the mass of the introduced sorbent on the ability to remove fluorine from solution was studied. The dose of the D1 and DMA sorbents was varied from 0.5 to 8.0 g/L. The fluorine extraction (%) by the D1 and DMA samples as a function of the mass of the added sorbent is shown in Fig. 2.

It is evident from Fig. 2 that an increase in the mass of the two sorbents is accompanied by an increase in the fluorine extraction. The concentration of surface hydroxyl groups is related to the sorbent concentration through the density of surface sites; therefore, the fluorine extraction percentage increases with increasing sorbent dose. It should be noted that, in the entire weight range, the fluorine extraction by the DMA sample is more than two times higher than the fluorine extraction by D1. Initially, at a DMA sorbent dose of 0.8 g/L, the fluorine extraction abruptly increases to 65.6%; then it increases more gradually and achieves 90% at a dose of 2.0 g/L. A further addition of the sorbent does not have a significant effect on the fluorine extraction. This fact made it possible to assume that this value is optimum for all further experiments. A similar tendency is observed for the D1 sample. An increase in the D1 sorbent weight to more than 2.0 g/L does not considerably improve the fluorine extraction either; this weight was selected for further use in adsorption experiments.

The ability of the sorbent to bind the adsorbate can be estimated using distribution coefficient K_d, which is dependent on the pH and the surface type and can be calculated as follows:

$$K_d = \frac{C_s}{C_e}. \quad (1)$$

Here, C_s is the fluoride concentration in the solid phase (mmol/L) and C_e is the fluoride concentration in the equilibrium solution (mmol/L). The distribution coefficient value increases with added sorbent weight, as evidenced by the dependence shown in Fig. 3.

At a given solution pH, an increase in $\log K_d$ is an indirect indication of a heterogeneity of the DMA surface because this parameter is constant in the case of a homogeneous surface [52].

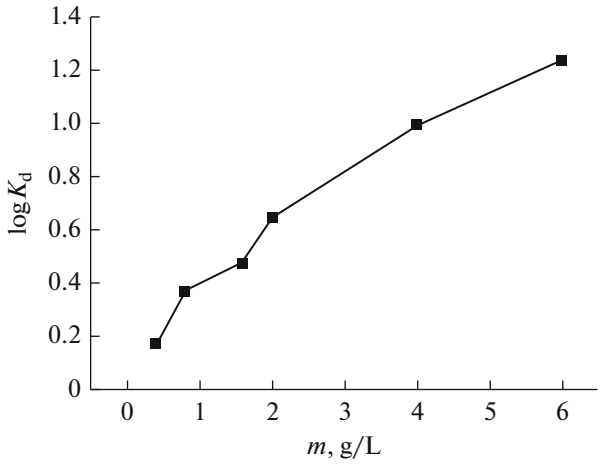

Fig. 3. Dependence of distribution coefficient K_d for the fluorine adsorption by DMA on the sorbent weight.

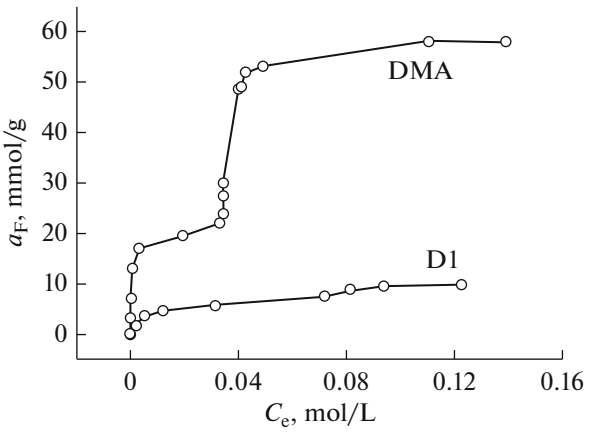

Fig. 4. Experimental isotherms of fluorine adsorption from an acetate buffer by the D1 and DMA samples at 20°C, a pH of 4.8, and a sorbent dose of 2.0 g/L.

Effect of Initial Fluorine Concentration on Adsorption

Figure 4 shows the fluorine adsorption isotherms for the D1 and DMA samples from an acetate buffer at optimum parameters and room temperature.

Visual analysis suggests that these isotherms have two well-defined steps.

The resulting two-step adsorption isotherms cannot be described using equations of the most common adsorption models, i.e., Freundlich or Langmuir equations. Therefore, in this case, a two-step model derived by the summation of Langmuir-type isotherms was used. Thus, each step in the isotherm can be described by the Langmuir equation [53]:

$$a = \frac{a_m K_L C}{1 + K_L C}. \quad (2)$$

Hereinafter, a is the amount of fluorine adsorbed per gram of sorbent at equilibrium, mmol/g; a_m is the adsorption capacity of the sorbent at saturation, mmol/g; C is the equilibrium fluorine concentration in solution, mmol/L; and K_L is the adsorption equilibrium constant, L/mmol.

The authors of [41] introduced the concept of a critical (limiting) concentration of a substance adsorbed on a sorbent, which is dependent on the adsorbent–adsorbate interaction. It is assumed that, above this concentration, a new adsorption layer is formed and another new adsorption mechanism becomes effective. Taking into account the limiting concentration, Eq. (2) can be rewritten as follows:

$$a = \frac{a_m K_L (C - b)}{1 + K_L (C - b)}, \quad (3)$$

where b is the limiting concentration, mmol/L.

In the physical and mathematical sense, this function can be used provided that $C > b$. Thus, Eq. (3) can be modified with a new function which is zero if the concentration of the starting material is lower than the critical concentration; in the range of higher concentrations, it is a linear function of the initial concentration of the substance:

$$\left[\frac{(C-b) + abs(C-b)}{2}\right] = C - b, \text{ if } C - b > 0, \text{ and}$$

$$\left[\frac{(C-b) + abs(C-b)}{2}\right] = 0, \text{ if } C - b \le 0.$$

Hence, Eq. (3) can be rewritten as follows:

$$a = \frac{a_m K_L \left[\frac{(C-b) + abs(C-b)}{2}\right]}{1 + K_L \left[\frac{(C-b) + abs(C-b)}{2}\right]}. \quad (4)$$

After transformations, Eq. (4) yields

$$a = \frac{a_m K_L [(C-b) + abs(C-b)]}{2 + K_L [(C-b) + abs(C-b)]}. \quad (5)$$

This mathematical formula describes the one-step model for one type of adsorption mechanism.

For the calculation of the second and subsequent steps, it is assumed that the total adsorption capacity is the sum of the adsorption capacities of effective adsorption sites above the critical concentration. In this theory, general terms are adsorption equilibrium constant K, adsorption capacity a_m, and limiting equilibrium concentration b (provided that the adsorption occurs by the mechanism under discussion).

A two-step isotherm will be as follows:

$$a = \frac{a_{m_1} K_{L_1} C}{1 + K_{L_1} C} + \frac{a_{m_2} K_{L_2} [(C - b_2) + abs(C - b_2)]}{2 + K_{L_2} [(C - b_2) + abs(C - b_2)]}. \quad (6)$$

Parameter b_1 is irrevocably zero in the first step.

Table 4. Parameters of Eq. (6) of the two-step fluorine adsorption isotherm of the D1 and DMA samples

Sample	a_{m1}, mmol/g	a_{m2}, mmol/g	K_{L1}, L/mmol	K_{L2}, L/mmol	b_2, L/mmol
D1	6.30	3.62	0.178	0.276	65.0
DMA	7.86	23.60	0.333	0.318	33.3

This mathematical expression was used to describe the two-step fluorine adsorption isotherms of the D1 and DMA samples. The calculated adsorption parameters are listed in Table 4.

The isotherms plotted according to Eq. (6) and Table 4 are shown in Fig. 5.

It is evident from Fig. 5 that the two-step Langmuir isotherm model accurately describes the experimental data on the fluorine adsorption by the diatomite samples from solutions with a high initial concentration.

Adsorption Mechanism

The slope of the initial portions of the adsorption isotherms recorded under equilibrium conditions characterizes the intensity of the adsorbent–adsorbate interaction and the degree of utilization of sorbents; the adsorption isotherm shape can indicate the mechanism of adsorption (whether it is chemical or physical), while the specific equilibrium adsorption magnitude makes it possible to determine the sorbent dose for adsorption under static conditions.

The sorption isotherm shape suggests the occurrence of a sorbate–sorbent interaction, but does not confirm this information. It can be assumed that the steps ascending in isotherms indicate the heterogeneity of the active surface of the adsorbent. A smaller portion of the active sites can exhibit a high activity; they are saturated at relatively low concentrations. The diversity of the chemical heterogeneity of the studied adsorbent is also complicated by the colloidal structure of the aluminosilicate comprising micro- and mesopores in addition to the existence of macropores in the diatomite.

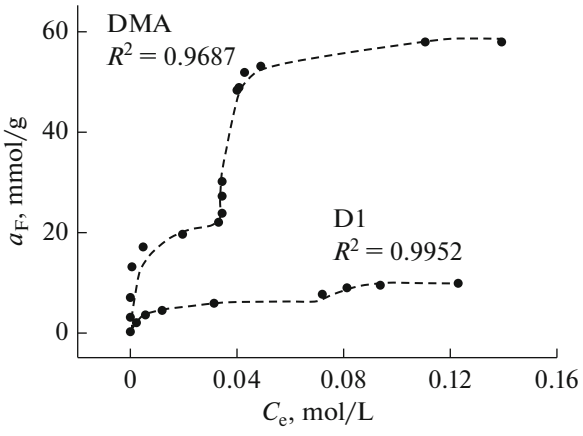

Fig. 5. Fluorine adsorption isotherms of the D1 and DMA samples: the points stand for the experimental results; the dashed lines denote the data calculated according to Eq. (6) and Table 4.

Consider the fluorine adsorption isotherm of the DMA sample. It should be noted that, if the equilibrium fluorine concentration is lower than 0.033 mol/L, the curve forms a Langmuir-type isotherm, which involves the filling of active sites by individual molecules (ions). In this case, the almost vertical initial portion of the isotherm indirectly indicates a very high affinity of the adsorbate to the adsorbent and implies the formation of a chemical bond between the interacting substances. If the specific amount of adsorbed fluorine (a_m) is 22.3 mmol/g, then it is assumed that the adsorbent surface is covered by individual molecules of the resulting compound (maximum adsorption capacity a_{m1}). After that, a second layer is formed; the surface concentration is zero again; the adsorption involves new sites; this feature implies a different type of interaction. The amount of adsorbed fluorine abruptly increases, while the equilibrium concentration hardly increases at all. In this case, the curve shape also suggests the occurrence of a chemical interaction. Thus, in a range of equilibrium concentrations of 0.033–0.040 mol/L, the entire adsorbed fluorine is absorbed by the surface sites to form a new compound. After that, when all of the available reaction sites are exhausted and the surface is saturated again, the equilibrium concentration begins to increase, while the adsorption abruptly slows down. The second step of the isotherm has a maximum adsorption capacity a_{m2} of about 58 mmol/g.

It is easy to select two fluorine–aluminum compounds with the lowest solubility—aluminum fluoride and cryolite (with negative logarithm pK_a of 19.0 and 33.84, respectively)—and assume the formation of these compounds on the surface and in the pores of DMA according to the following scheme:

$$Al^{3+} + 3F^- \rightarrow AlF_3,$$

$$AlF_3 + NaF \rightarrow NaAlF_4,$$

$$NaAlF_4 + 2NaF \rightarrow Na_3AlF_6.$$

At a high level of excess sodium fluoride in the solution, the resulting aluminum fluoride binds NaF to form a $NaAlF_4$ intermediate compound, which is transformed into cryolite owing to the further adsorption of NaF. Hence, it can be assumed that aluminum fluoride is formed at an equilibrium fluorine concentration of up to 0.033 M, while cryolite is formed in the second step.

To confirm this hypothesis, we used data on fluorine desorption from the D1 and DMA surfaces, X-ray

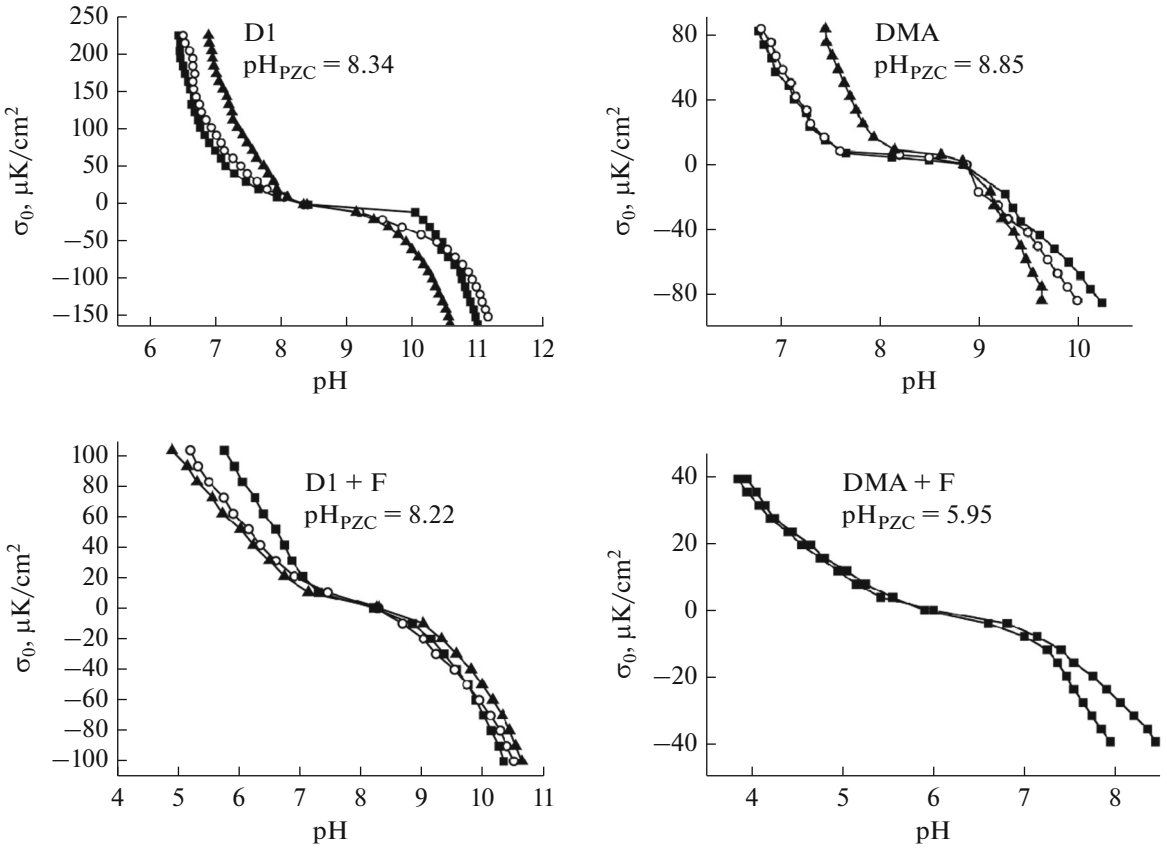

Fig. 6. Potentiometric titration curves of the D1 and DMA samples before and after fluorine adsorption.

diffraction and FTIR analysis results, and potentiometric titration data for D1 and DMA before and after fluorine adsorption by these samples.

Knowing the pH_{PZC} of the studied material, it is possible to obtain information about the possible attraction or repulsion between the sorbent and the sorbate and provide the conditions required for the effective implementation of adsorption [54].

Figure 6 shows the potentiometric titration curves of D1 and DMA before and after fluorine adsorption. The intersection of the three curves with the *X* axis gives the PZC (pH_{PZC}); in this study, it is 8.34 and 8.85 for the D1 and DMA samples, respectively.

At the pH_{PZC}, the total charge of cations and anions on the sample surface is zero.

The titration curves show that an increase in pH leads to a decrease in the density of the positive surface charge. The surface charge is positive if the solution pH is lower than pH_{PZC} and negative if the pH is higher than pH_{PZC}; that is, the ability of the sorbent to adsorb negatively charged fluorine anions increases in the acidic pH range.

Owing to the modification-induced formation of new aluminosilicate compounds on the diatomite surface, the pH_{PZC} of DMA is shifted to higher values. Aluminosilicates can be regarded as silicates in which some of the silicon–oxygen tetrahedra SiO_4^{4-} are replaced by aluminum–oxygen tetrahedra AlO_4^{5-} [55]. The partial substitution of Al atoms for Si atoms in silicates, owing to their different valences, generates an excess negative charge, which is compensated by the introduction of Na^+, K^+, Mg^{2+}, or Ca^{2+} cations (less frequently, Ba^{2+} and Li^+) into the aluminosilicate crystal lattice [56]. An increase in the Al/Si ratio leads to a decrease in the aluminosilicate ion sizes and an increase in the total negative charge per aluminum atom [57]; as a result, the sorbent surface in solution adsorbs a larger number of protons and the pH_{PZC} is shifted to higher values [58].

The fluorine adsorption mechanism can be comprehensively understood if one takes into account the change in pH_{PZC} after adsorption. It is known that the formation of inner-sphere complexes (chemisorption) between a metal cation located at exchange positions in the sorbent structure and anionic compounds from the solution leads to a shift of the pH_{PZC} of the final product to a more acidic range; this fact confirms the formation of some acid groups on the sorbent surface. Specifically sorbed (chemisorbed) substances contrib-

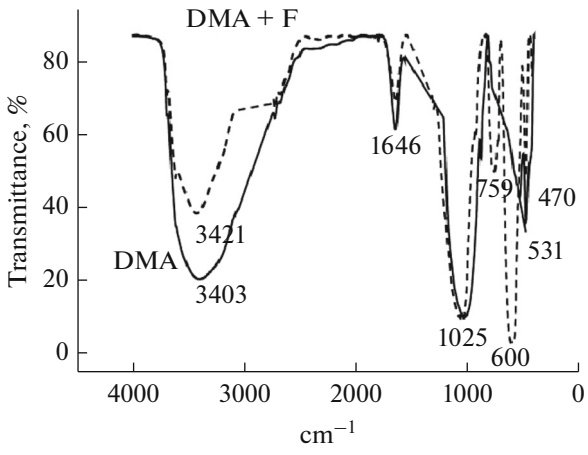

Fig. 7. FTIR spectra of the DMA sample before and after fluorine adsorption.

ute to a shift of the pH_{PZC} of the adsorbent surface after adsorption. If a cation is chemisorbed, pH_{PZC} is shifted to higher values; in the case of chemisorption of an anion, pH_{PZC} is shifted to a more acidic region [59, 60].

Fluorine absorption by aluminol sites of a positively charged surface at $pH < pH_{PZC}$ is attributed to a two-step mechanism, i.e., protonation/exchange of ligands and surface intraspheric complexation [34]:

$$AlOH_s + H^+ \rightarrow AlOH_2^+$$

$$AlOH_2^+ + F^- \rightarrow AlF_s + H_2O$$

Overall reaction:

$$AlOH_s + H^+ + F^- \rightarrow >AlF_s + H_2O.$$

This reaction provides an explanation to the decrease in the density of the positive charge on the sorbent surface under these conditions. In addition, the surface hydroxyls are replaced by fluoride ions; the entire charge of the fluorine (–1) is concentrated on the surface [61, 62]; this finding is consistent with our measurements of pH_{PZC}.

After adsorption, the pH_{PZC} of the D1 sample is also slightly shifted to a more acidic region; this fact indicates the formation of a chemical compound. The data on the composition of D1 (Table 1) suggest that fluorine interacts with calcium, which is contained in the sample in a significant amount (about 12% in the form of calcite), to form CaF_2 according to the reaction

$$Ca^{2+}_{(s)} + 2F^-(aq) \rightarrow CaF_{2(s)}.$$

The potentiometric titration results are confirmed by the data on fluorine desorption. The sevenfold washing of the samples in a buffer solution showed that the amount of fluorine desorbed from the surface of D1 and DMA is 69 and 3.2%, respectively; this finding suggests that the remaining fluorine is bound to the surface active sites of the adsorbent via chemical bonding.

The identification of the resulting compounds was conducted using the FTIR analysis data (Figs. 7, 8).

The absorption lines peaking at 3403 cm^{-1} (region of 3550–3200 cm^{-1}) and 1646 cm^{-1} correspond to the stretching and bending vibrations of the O–H bond of the surface OH^- groups and molecular water, respectively [63]; the peaks at 1025 and 531 cm^{-1} can be assigned to the stretching and bending vibrations of the Si–O–Al bond in aluminosilicate; the line peaking at 470 cm^{-1} is attributed to the bending vibrations of the Si–O bond in diatomite [64–66].

The FTIR spectra of the sample after fluorine adsorption show a decrease in the intensity of the peaks characteristic of hydroxyl ions and molecular water and the occurrence of new absorption lines with wave numbers of 759, 400, and 600 cm^{-1}, which corre-

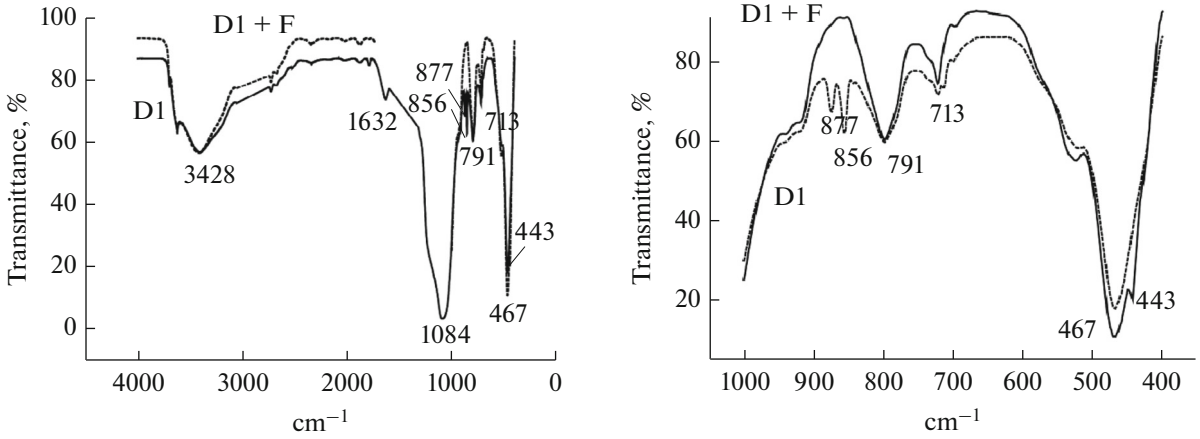

Fig. 8. FTIR spectra of the D1 sample before and after fluorine adsorption. The right panel shows a magnified scale up to 1000 cm^{-1}.

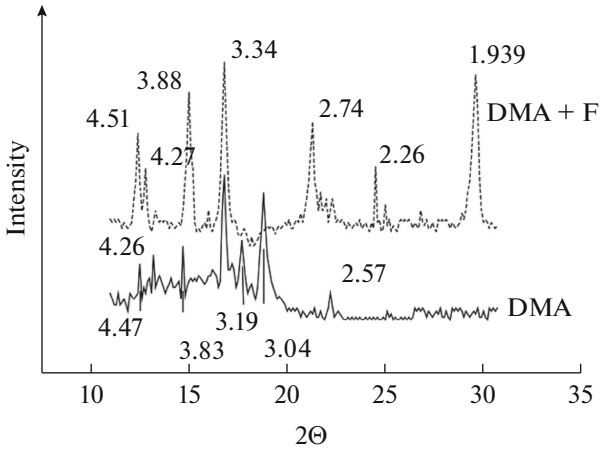

Fig. 9. X-ray diffraction patterns of the DMA sample before and after fluorine adsorption.

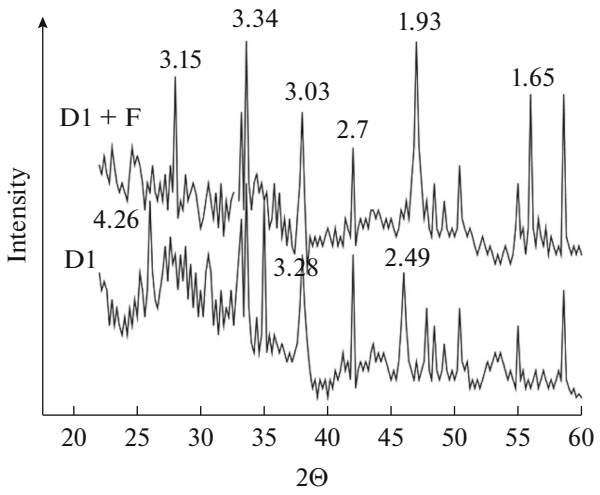

Fig. 10. X-ray diffraction patterns of the D1 sample before and after fluorine adsorption.

spond to the stretching and symmetric stretching vibrations of the Al–F bond; the strong signal at 600 cm^{-1} corresponds to vibrations of the Al–F bond in cryolite (AlF_6^{3-}) [67–69].

A decrease in the intensity of the peaks at 3403 and 1646 cm^{-1} suggests that the adsorption process involves hydroxyl groups and occurs by the ion-exchange mechanism; this finding is consistent with the data on fluorine adsorption without any buffer and the increase in the solution pH from 7.5 to 11.5 (Table 2). The disappearance of the line at 531 cm^{-1} can be attributed to the involvement of the Si–O–Al bond in the adsorption of fluoride ions. The appearance of new peaks characteristic of aluminum–fluorine compounds suggests that the fluorine absorption by the DMA sample occurs owing to the complexation of fluoride ions with aluminum; in other words, fluorine is chemically sorbed on DMA. Similar observations can be found in the literature on fluorine removal by aluminum-containing sorbents. Thus, the authors of [70] confirmed that the fluorine adsorption by aluminum titanate and bismuth aluminate occurs by the chemisorption mechanism through the formation of new Al–F bonds.

Wang et al. [71] showed that the fluorine adsorption by aluminum hydroxide at low pH values ($pH < pH_{PZC}$) can occur by a two-step mechanism—the protonation of surface Al–O groups with ligand exchange and the subsequent formation of an Al–F chemical bond [72, 21].

In the spectra of the D1 sample (Fig. 8), the absorption lines peaking at 877 and 856 cm^{-1}, which correspond to the bending vibrations of the CO_3^{2-} group of calcite contained in the D1 sample [63], disappear after fluorine adsorption. The shoulder with a maximum at 443 cm^{-1} can be attributed to the stretching vibrations of the Ca–F bond in CaF_2 [73]. The absorption lines of hydroxyl ions and water with peaks at 3428 and 1632 cm^{-1} do not undergo any visible changes; this feature can be attributed either to the fact that they are not involved in adsorption or to the buffer capacity of silicate ions. The absorption bands of stretching and bending vibrations of the Si–O bond at 1084, 791, 713, and 467 cm^{-1} remain unchanged after fluorine adsorption.

The formation of new compounds after fluorine adsorption by the D1 and DMA samples can also be observed in the diffraction patterns of the samples (Figs. 9, 10).

In the X-ray diffraction pattern of the DMA sample after fluorine adsorption, the intensity of the diffraction reflections of aluminosilicate with interplanar distances of 2.57, 3.04, and 3.19 Å decreases; they almost disappear, being replaced by new lines with interplanar distances of 1.94, 2.26, 2.74, 3.88, and 4.51 Å, which are characteristic of a cryolite phase [74, 75]. This finding confirms that the absorption of fluoride ions by the DMA surface occurs by the chemisorption mechanism, which apparently changes the adsorbent structure. The occurrence of an interaction between the fluoride ions and the aluminum to form new Al–F bonds is evidenced by the appearance of new peaks in the diffraction patterns after adsorption. Hence, it has been confirmed that, in our study, fluorine is chemically adsorbed through the formation of Al–F complexes.

Analysis of the diffraction pattern of the D1 sample before and after fluorine adsorption confirms the involvement of calcite in the adsorption process and the formation of fluorite. The diffraction reflections of calcite with interplanar distances of 4.26, 3.39, 3.28, and 2.49 Å disappear; new lines characteristic of fluorite with $d = 3.15$, 1.93, and 1.65 Å appear; the lines of silica with $d = 3.34$, 3.03, 2.70 Å, etc., remain unchanged [73, 76].

Hence, the fluorine adsorption by D1 occurs with the involvement of calcite, the replacement of the carbonate group by fluorine, and the formation of a CaF_2 chemical compound.

CONCLUSIONS

Fluorine removal by the D1 and DMA samples from solutions containing 0.01–0.3 mol/L of fluorine has been studied. Experiments have been conducted under static conditions at room temperature.

It has been shown that the pH value plays an important role in the fluorine removal from water. The optimum pH for the fluorine adsorption by DMA is 4.5–5.5.

The maximum capacity of the sorbents has been determined; at an initial fluorine concentration in water of 0.3 mol/L, it is about 58 mmol/g for the DMA sample; this value is 5.5 times higher than that of the D1 sample, which is 9.7 mmol/g.

To determine the adsorption capacity of the samples with respect to fluorine, the dependence of adsorption on the solution pH, initial fluorine concentration, sorbent weight, and sorption time has been studied.

Fluorine adsorption isotherms of these samples have been recorded. Equilibrium adsorption data have been modeled using a two-step Langmuir model; it has been shown that the experimental data on fluorine adsorption are in good agreement with the data calculated according to this model: correlation coefficient R^2 is 0.9952 and 0.9687 for the D1 and DMA samples, respectively.

The mechanism of fluorine adsorption by the studied samples has been analyzed.

It has been shown that one of the major components of the mechanism of fluorine adsorption by DMA is the exchange of ligands with the surface –OH groups to form aluminum fluoride AlF_3. At high initial concentrations of fluorine, the adsorption observed above the first plateau is the result of precipitation of fluoride in the form cryolite Na_3AlF_6, along with other sorption mechanisms, particularly the adsorption of fluorine in the form of AlF_4^-, via capturing the Al–F compounds from the interparticle liquid inside the pores, and the surface precipitation of cryolite and other fluorine–aluminum compounds. The fluorine adsorption by D1 also occurs through chemisorption and the formation of a calcium–fluorine compound—CaF_2—on the surface and in the pores of the sorbent.

ACKNOWLEDGMENTS

This work was performed under institutional project no. 11.817.05.04A and MIS-ETC 1443 project no. 2.2.1.74459.339.

REFERENCES

1. *Fluoride: Exposure and Relative Source Contribution Analysis*, Washington, DC: US Environ. Prot. Agency, 2010. http://water.epa.gov/action/advisories/drinking/upload/fluoridereport.pdf.
2. Tewari A. and Dubey A., *J. Chem. Pharm. Res.*, 2009, vol. 1, no. 1, pp. 31–37.
3. *Guidelines for Drinking-Water Quality First Addendum to Third Edition*, Vol. 1: *Recommendations*, Geneva: World Health Org., 2006.
4. *Fluoride in Drinking Water: A Scientific Review of EPA's Standards*, Washington, DC: Natl. Acad. Press, 2006.
5. Renuka, P. and Pushpanjali, K., *Int. J. Eng. Sci.*, 2013, vol. 2, no. 3, pp. 86–94.
6. Yang, C.-L. and Dluhy, R., *J. Hazard. Mater. B*, 2002, vol. 94, pp. 239–252.
7. Ingle, N.A., Dubey, H.V., Kaur, N., and Sharma, I., *J. Health Res. Rev.*, 2014, vol. 1, pp. 1–4.
8. Gill, T., Tiwari, S., and Kumar, P.A., *Int. J. Environ. Res. Dev.*, 2014, vol. 4, no. 2, pp. 179–182.
9. Madhukar, M., Murthy, B.M.S., and Udayashankara, T.H., *J. Water Pollut. Purif. Res.*, 2014, vol. 1, no. 2, pp. 1–12.
10. Mohapatra, M., Anand, S., Mishra, B.K., Giles, D.E., and Singh, P., *J. Environ. Manage.*, 2009, vol. 91, pp. 67–77.
11. Mulugeta, E., Zewge, F., Johnson, C.A., and Chandravanshi, B.S., *Water SA*, 2015, vol. 41, no. 1, pp. 121–128.
12. Shrivastava, A.K. and Sharma, M.K., *Sci. Rev. Chem. Commun.*, 2012, vol. 2, no. 2, pp. 133–140.
13. Rafique, A., Awan, M.A., Wasti, A., Qazi, I.A. and Arshad, M., *J. Chem.*, 2012, vol. 10, pp. 1–7.
14. Abe, I., Iwasaki, S., Tokimoto, T., Kawasaki, N., Nakamura, T. and Tanada, S., *J. Colloid Interface Sci.*, 2004, vol. 275, pp. 35–39.
15. Nasr, B., Walha, K., Puel, F., Mangin, D., Amar, R.B., and Charcosse, C., *Desalin. Water Treat.*, 2014, vol. 52, nos. 10–12, pp. 2231–2240.
16. Togarepi, E., Mahamadi, C. and Mangombe, A., *Afr. J. Environ. Sci. Technol.*, 2012, vol. 6, no. 3, pp. 176–181.
17. Tiwary, K.K., Shrivastava, A.K., Mishra, S., and Jha, R.R., *EJEAFChe, Electron. J. Environ., Agric. Food Chem.*, 2011, vol. 10, no. 11, pp. 3104–3112.
18. Mahramanlioglu, M., Kizilcikli, I., and Bicer, I.O., *J. Fluorine Chem.*, 2002, vol. 115, pp. 41–47.
19. Coetzee, P.P., Coetzee, L.L., Puka, R. and Mubenga, S., *Water SA*, 2003, vol. 29, no. 3, pp. 331–338.
20. Lavecchia, R., Medici, F., Piga, L., Rinaldi, G., and Zuorro, A., *Chem. Eng. Trans.*, 2012, vol. 26, pp. 225–230.
21. Agarwal, M., Rai, K., Shrivastav, R. and Das, S., *Water, Air, Soil Pollut.*, 2002, vol. 141, pp. 247–261.
22. Bakr, H.E.G.M.M., *Asian J. Mater. Sci.*, 2010, vol. 2, no. 3, pp. 121–136.
23. Xu, L., Gao, X., Li, Z., and Gao, C., *Desalination*, 2015, vol. 369, pp. 97–104.
24. Janta, S., Watanesk, S., Watanesk, R., and Thiansem, S., *Adv. Mater. Res.*, 2008, vols. 55–57, pp. 865–868.
25. Da Conceição, V.M., Bonicontro, M.C., Ugri, A., Silveira, C., et al., *Can. J. Chem. Eng.*, 2015, vol. 93, no. 1, pp. 37–45.

26. Ramesh, S.T., Gandhimathi, R., Nidheesh, P.V. and Taywade, M., *Environ. Res., Eng. Manage.*, 2012, vol. 2, no. 60, pp. 12–20.
27. Onyango, M.S., Kojima, Y., Aoyi, O., Bernardo, E.C., and Matsuda, H., *J. Colloid Interface Sci.*, 2004, vol. 279, pp. 341–350.
28. Harikumar, P.S.P., Jaseela, C., and Megha, T., *Nat. Sci.*, 2012, vol. 4, no. 4, pp. 245–251.
29. Zelentsov, V.I., Datsko, T.Ya. and Dvornikova, E.E., *Surf. Eng. Appl. Electrochem.*, 2008, vol. 44, no. 1, pp. 64–68.
30. Zelentsov, V. and Datsko, T., *Mold. J. Phys. Sci.*, 2006, vol. 5, no. 2, pp. 162–168.
31. Datsko, T.Ya., Zelentsov, V.I. and Dvornikova, E.E., *Prot. Met. Phys. Chem. Surf.*, 2011, vol. 47, no. 3, 295–301.
32. Zelenţov, V., Daţko, T., and Dvornikova, E., *MD 3973C2* (State Standard) *2010-07-31: Procedeu de obţinere a sorbentului pebaza de diatomit pentru purificare de ionii de fluor.*
33. *MD 657C2* (State Standard) *2014-02-28. Procedeu de purificare a apei de ioni de fluor şi acizi humici*.
34. Datsko, T. and Zelentsov, V., *Sci. Ann. Danube Delta Inst.*, 2014, vol. 20, pp. 51–57.
35. Lv, L., He, J., Wei, M., Evans, D.G., and Zhou, Z., *Water Res.*, 2007, vol. 41, pp. 1534–1542.
36. Harrington, L.F., Cooper, E.M. and Vasudevan, D., *J. Colloid Interface Sci.*, 2003, vol. 267, pp. 302–313.
37. Sposito, G., *The Chemistry of Soils*, New York: Oxford Univ. Press, 1989.
38. Evangelou, V.P., *Environmental Soil and Water Chemistry: Principles and Applications*, New York: Wiley, 1998.
39. Gregg, S.J. and Jacobs, J., *Trans. Faraday Soc.*, 1948, vol. 44, pp. 574–588.
40. Brunauer, S., Deming, L.S., Deming, W.E. and Teller, E., *J. Am. Chem. Soc.*, 1940, vol. 62, pp. 1723–1732.
41. Konda, L.N., Czinkota, I., Fuleky, G. and Morovjan, G. J., *Agric. Food Chem.*, 2002, vol. 50, pp. 7326–733.
42. Tolner, L., The determination of parameters of multistep, *Appl. Ecol. Environ. Res.*, 2008, vol. 6, no. 4, pp. 111–119.
43. Konda, L.N., Investigation of sorption behavior of organic pesticides on soil, *PhD Thesis*, Gödöllő, Hungary, 2002. http://phd.szie.hu/JaDoX_Portlets/documents/document_3310_section_3704.pdf.
44. Parks, G.A., Surface energy and adsorption at mineral/water interfaces: An introduction, in *Mineral-Water Interface Geochemistry: Reviews in Mineralogy*, Washington, DC: Mineral. Soc. Am., 1990, vol. 23, pp. 133–175.
45. Lewis-Russ, A., Measurement of surface charge of inorganic geological materials—techniques and their consequences, in *Advances in Agronomy*, Sparks, D.L., Ed., New York: Academic, 1991, vol. 46, pp. 199–243.
46. Parks, G.A. and de Bruyn, P.L., *J. Phys. Chem.*, 1962, vol. 66, pp. 967–973.
47. Yopps, J.A. and Fuerstenau, D.W., *J. Colloid Sci.*, 1964, vol. 19, no. 1, pp. 61–71.
48. Samson, H.R., *Clay Miner.*, 1952, vol. 1, no. 8, pp. 266–271.
49. Datsko, T.Ya., Zelentsov, V.I. and Dvornikova, E.E., *Surf. Eng. Appl. Electrochem.*, 2011, vol. 47, no. 6, pp. 530–539.
50. Zhu, M.-X., Xie, M., and Jiang, X., *Appl. Geochem.*, 2006, vol. 21, pp. 675–683.
51. Nordin, J.P., Sullivan, D.J., Phillips, B.L., and Casey, W.H., *Geochim. Cosmochim. Acta*, 1999, vol. 63, no. 21, pp. 3513–3524.
52. Tor, A., *Desalination*, 2006, vol. 201, pp. 267–276.
53. Langmuir, I., *J. Am. Chem. Soc.*, 1916, vol. 38, pp. 2221–2295.
54. Fiol, N. and Villaescusa, I., *Environ. Chem. Lett.*, 2009, vol. 7, pp. 79–84.
55. Yuan, P., Wu, D.Q., He, H.P. and Lin, Z.Y., *Appl. Surf. Sci.*, 2004, vol. 227, pp. 30–39.
56. Wada, S.I. and Wada, K., *J. Soil Sci.*, 1980, vol. 31, pp. 457–467.
57. Jara, A.A., Goldberg, S., and Mora, M.L., *J. Colloid Interface Sci.*, 2005, vol. 292, pp. 160–170.
58. Inoue, K. and Satoh, C., *Clay Clay Miner.*, 1992, vol. 40, no. 3, pp. 314–318.
59. Tombácz, E., *Chem. Eng.*, 2009, vol. 53, no. 2, pp. 77–86.
60. James, R.O. and Parks, G.A., *Surf. Colloid Sci.*, 1982, vol. 12, pp. 119–216.
61. Reyes, B.J.L., Robledo, C.A., López, V.A., and Herrera, U.R., *Sep. Sci. Technol.*, 2002, vol. 37, no. 8, pp. 1973–1987.
62. Hiemstra, T. and van Riemsdijk, W.H., *J. Colloid Interface Sci.*, 2000, vol. 225, pp. 94–104.
63. Nayak, P.S. and Singh, B.K., *Bull. Mater. Sci.*, 2007, vol. 30, no. 3, pp. 235–238.
64. Bhaskar, J.S. and Gopalakrishnarao, P., *J. Mod. Phys.*, 2010, vol. 1, pp. 206–210.
65. Marel, H.M.V. and Bentelspacher, H., *Atlas of Infrared Spectroscopy of Clay Minerals and Their Admixtures*, New York: Elsevier, 1976.
66. Hubicki, Z., Zieba, E., Wojcik, G. and Ryczkowski, J., *Acta Phys. Pol. A*, 2009, vol. 116, no. 3, pp. 312–314.
67. Yu, J., Bai, H., Wang, J., Li, Z., et al., *New J. Chem.*, 2013, vol. 37, pp. 366–372.
68. Grorelny, M., *J. Fluorine Chem.*, 1976, vol. 8, pp. 353–362.
69. Fletcher, H.R., Smith, D.W., and Pivonka, P., *J. Environ. Eng.*, 2006, vol. 132, pp. 229–246.
70. Karthikeyan, M. and Elango, K.P., *J. Environ. Sci.*, 2009, vol. 21, pp. 1513–1518.
71. Wang, S.-G., Ma, Y., Shi, Y.-J., and Gong, W.-X., *J. Chem. Technol. Biotechnol.*, 2009, vol. 84, pp. 1043–1050.
72. Ayoob, S., Gupta, A.K., Bhakat, P.B., and Bhat, V.T., *Chem. Eng. J.*, 2008, vol. 140, pp. 6–14.
73. Tahvildari, K., Esmaeilipour, M., Ghammamy, Sh., and Nabipour, H., *Int. J. Nano Dimens.*, 2012, vol. 2, no. 4, pp. 269–273.
74. Simko, F. and Boca, M., *Helv. Chim. Acta*, 2007, vol. 90, pp. 1529–1537.
75. Rosenberg, P.E., *Can. Mineral.*, 2006, vol. 44, pp. 125–134.ì
76. Khunur, M.M., Risdianto, A., Mutrofin, S., and Prananto, Y.P., *Bull. Chem. React. Eng. Catal.*, 2012, vol. 7, no. 1, pp. 71–77.

Translated by M. Timoshinina